AIChE WILEY InterScience DISCOVER SOMETHING GREAT

MATERIALS, INTERFACES, AND ELECTROCHEMICAL PHENOMENA

Regulation of Tack Development of Acrylate Films by the Properties of the Support

Gregory M. Fike and Sujit Banerjee
Institute of Paper Science and Technology, School of Chemical and Biomolecular Engineering, Georgia Institute of Technology, Atlanta, GA 30332

DOI 10.1002/aic.10814
Published online March 24, 2006 in Wiley InterScience (www.interscience.wiley.com).

Drying an acrylate formulation on carbon and stainless steel coupons leads to films with dramatic differences in tack. The tack of the film deposited on stainless steel is high, as expected, but that of the film on carbon steel is much lower. This difference arises from changes in the polar component of the surface energy. Atomic force microscopy showed that the carbon steel-based film had a rougher surface, and that the components separated into the valleys in the surface, thereby reducing the overall tack. The origin of the phenomenon lies in the nonuniformity of carbon steel. Local differences in heat transfer from the metal to the adjoining liquid layer gives rise to temperature differences at the surface of the film as it dries. This induces Marangoni flow, which leads to inhomogeneities in the composition and topology of the surface. © 2006 American Institute of Chemical Engineers *AIChE J,* 52: 2238–2242, 2006

Keywords: acrylate, tack, Marangoni, AFM, recycling, pressure sensitive adhesive

Introduction

The control of polymeric adhesives is important in the article industry because these contaminants can deposit on various process surfaces and cause plugging, picking, and other operational and product quality problems. The tack of polymeric adhesive films depends on their wettability,[1] surface roughness,[2,3] and viscoelastic behavior[4] among other properties. Wettability and roughness are important because the surface topology and surface chemistry control the degree of surface-to-surface contact. Increasing contact time and contact pressure have also been shown to alter the adhesive bond for rough surfaces by increasing the total contact area.[5] It follows that the viscoelastic behavior of the polymer plays a role in both the total contact area between the adhesive and substrate and also in the energy dissipation found during debonding.

We have found, surprisingly, that drying a commercial acrylate formulation on a stainless steel coupon leads to a tacky film (as expected), but a corresponding film deposited on carbon steel is almost completely nontacky. Thus, the adhesive properties of the film depend, in part, on the nature of the supporting metal. In this article we discuss the mechanism of the phenomenon.

Experimental

A commercial acrylate formulation (Carbotac 26171 from Noveon, 50% solids in water) was applied with a wire-wrapped metering rod as 20–40 μm films to 1008 carbon steel, and 304L stainless steel coupons precleaned with a variety of organic solvents. The roughness of the bare coupons was measured with profilometry, and with AFM to confirm that the initial surface topology was the same for both metal surfaces. The adhesive-coated coupons were dried in an oven at 25 to 130°C. Film thickness was measured with a magnetic thickness probe (CGX Gauge by Oxford Instruments, Elk Grove Village, IL). The relationship between film thickness and coating weight was linear, as expected, and resulted in adhesive layers that covered the substrates completely.

Atomic Force Microscopy (AFM) measurements were made with an MFP-3D instrument from Asylum Research (Santa Barbara, CA). Topological imaging used 240 μm long silicon cantilevers with spring constants of 1–2 N/m. The tack of the

Correspondence concerning this article should be addressed to S. Banerjee at sb@gatech.edu.

Table 1. Emissivities of Films Deposited on Various Coupons at Different Temperatures

Oven temperature (°C)	75	90	105
Heat flux (W/m^2)	200	241	321
Stainless steel emissivity (±0.03)	0.70	0.70	0.70
Carbon steel emissivity (±0.03)	0.36	0.34	0.46
Marked stainless steel emissivity (±0.03)	0.71	0.67	0.73

dry acrylate films was measured at room temperature with a Polyken tack tester from Testing Machines, Inc. (Islandia, NY). Here, a 5-mm stainless steel probe impacts the coupon and the force of separation is measured.

The temperature distribution of the surface of the coupons was measured during drying by infrared (IR) thermograpy with an AGEMA 900SW/TE system, comprised of a scanner equipped with a 40-degree FOV IR lens, and a high-speed system controller. The scanner detects radiation in the 2–5.4 μm range. The system is able to analyze images at the pixel level, and compensates for transmission through the atmosphere. IR imaging for temperature measurements requires a proper emissivity value. However, the emissivity is strongly dependent on the moisture content of the film, which complicates the measurement of absolute temperature. For this study, the emissivity of the drying film was determined by heating a bare stainless steel coupon with a known emissivity of 0.70 and simultaneously comparing the reading from a thermocouple in contact with the coupon to that of the IR camera. This provided the temperature profile of the coupons during heating. Emissivities of stainless and carbon steels are given in Table 1, along with the oven temperature and the heat flux. Experiments were also run with a stainless coupon marked with a "Sharpie" permanent marking pen in a 0.5 mm grid pattern such that about 50% of the surface of the coupon was covered by the ink. The purpose of marking the surface of the coupon is to interrupt the heat transfer from the coupon to the liquid film. The emissivity for this modified surface is also included in Table 1.

Results and Discussion

Tack and contact angle measurements

The tack of acrylate films prepared on carbon steel and stainless steel was very different. The film on the carbon steel surface resembles a piece of hard plastic, whereas that on the stainless steel surface was very tacky — as expected from a pressure sensitive adhesive. Tack values of films cured at different temperatures are shown in Figure 1. The tack of the adhesive dried on stainless steel was 2–5 N, whereas that of a film plated identically on carbon steel was an order-of-magnitude lower at 0–0.4 N. In both cases, the tack was independent of film thickness. Cleaning the metal surfaces with different solvent sequences prior to depositing the adhesive did not alter the results.

Static contact angles of water and methyl iodide on the films were then measured. The drops were placed on the surface, and an image was recorded as soon as the drop stopped oscillating and the contact angle was found from the image. The polar and nonpolar components of the surface energy calculated as per Fowkes[6] are illustrated in Figure 2. The overall surface energies of the two surfaces vary significantly at 41 N/m and 34 mN/m, for the carbon and stainless steel-based films, respectively. The nonpolar component remained about the same for both films, but the polar component was higher for the carbon-steel-based film, which is consistent with its absence of tack. The dependence on drying temperature was negligible. These trends were maintained across films in the thickness range of 22 – 42 μm.

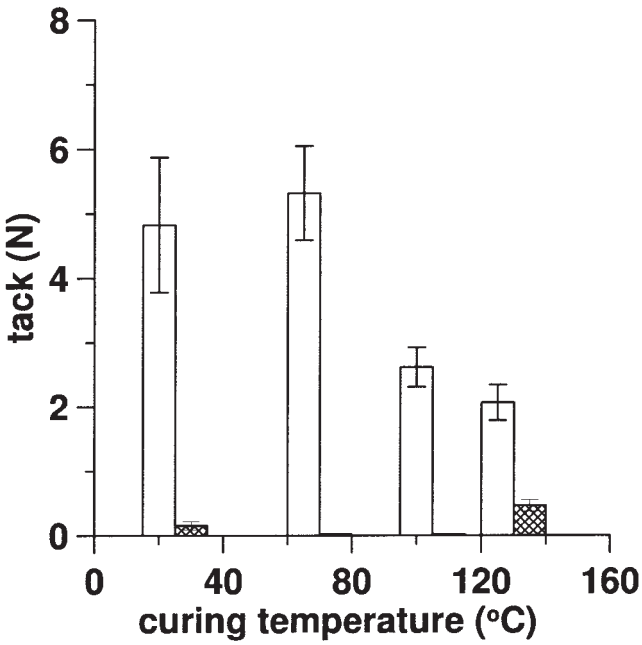

Figure 1. Tack of polyacrylate films dried on stainless steel (clear) and carbon steel (hatched) substrates.

The tack was measured with a 5-mm stainless steel probe. Values for the film on carbon steel at 80 and 120°C are negligible.

AFM measurements

The roughness of the films imaged with AFM over a series of increasing scan sizes is shown in Figure 3. Topological data are typically presented as root-mean square (rms) roughness, which is the standard deviation of height values collected over the scan. The plot includes results for "marked stainless steel" that will be discussed later. The roughness of the carbon steel film is clearly much greater than those of the other. Roughness

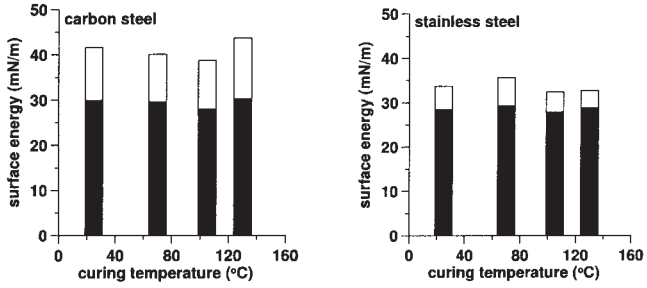

Figure 2. Surface energy components for a polyacrylate film deposited on carbon steel and stainless steel at various curing temperatures.

The black and clear bars represent nonpolar and polar components, respectively.

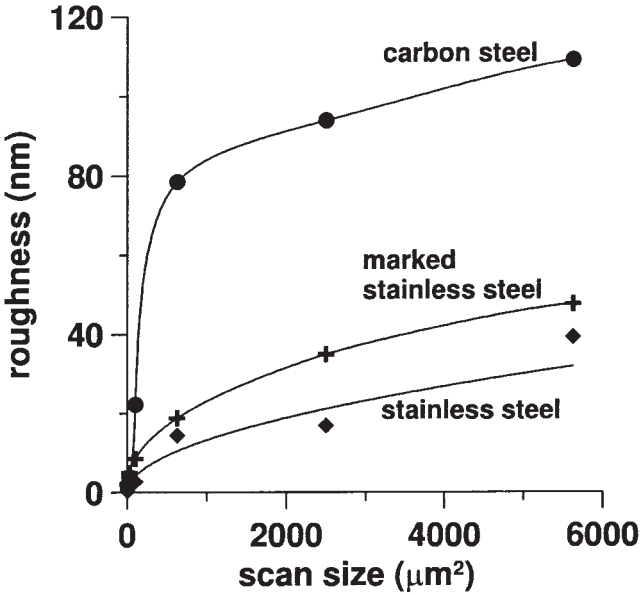

Figure 3. RMS roughness values for polyacrylate film on carbon steel and stainless steel at various scan sizes.

reduces tack by providing nucleation sites for cavity formation that eventually leads to bond failure. Other differences in properties between the two surfaces were revealed by tapping mode AFM. Here, the phase shift image indicates areas that dissipate energy differently. Figure 4 illustrates such an image of the tacky polymer surface on the stainless steel substrate. The darker areas are regions that are more attractive to the imaging tip. In contrast, the phase shift image for the carbon steel surface is clearly much rougher. The dark areas represent attractive regions of the surface that appear to have separated out, exposing large areas of less attractive material.

Figure 5 combines phase shift and topographical images for the film on carbon steel. The topography is presented as the vertical axis in the image. The color scale is taken from the phase shift images and the darker colors again represent softer, more attractive portions of the film. These images provide the strongest support for the nontacky nature of the film. The attractive, sticky material is segregated in the valleys, which makes it less accessible to the tack probe. The probe only contacts the lighter areas that are less attractive and of lower tack. The tack of these materials was measured by contact mode AFM. The pull-off force (F_p) is basically a tack measurement performed with the tip of the AFM cantilever. New

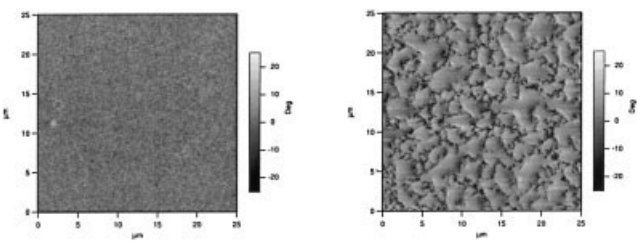

Figure 4. 25 μm phase shift scan of polyacrylate film on stainless steel (left), and carbon steel (right).

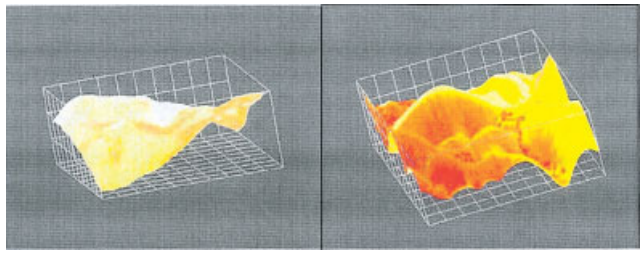

Figure 5. AFM image of a polyacrylate film on carbon steel (left) and stainless steel (right).

The surface contour is the height scan and the color scheme is the phase-shift scan with the dark colors representing sticky material. The images are 25 μm on each side and the height ranges from -60 to 60 nm.

tips were used for each measurement to reduce the likelihood of tip damage or contamination affecting subsequent measurements. The tips used in this experiment were of tetrahedral shape with an average tip radius of 10 nm. The F_p for the less attractive regions located at the high points of the topography was 21 ± 7 nN/100 nm^2; that for the attractive, darker regions contained in the valleys of the topography was 68 ± 18 nN/100 nm^2. These results are consistent with the surface energy result, where the polar component of the surface energy is higher for the film on carbon steel.

Drying measurements

The development of the rougher surface for the carbon-steel based film was studied through IR thermography of the films as they dried. We have previously shown that the coefficient of variation (COV) of the average surface temperature of a wet surface as it dries is a good measure of surface roughness.[7] Uneven films give rise to greater temperature variation across the surface because of differences in evaporative cooling, which is reflected by a higher COV. COV profiles during drying in a 117°C oven are compared for carbon — and stainless-coated films in Figure 6; the COV for the former is clearly higher. The COV of the surface temperature from heating the bare metal itself was also determined. A silicon wafer was included as a reference, because these wafers are known to have a uniform surface. A thermal image comprised of about 500 50-μm pixels was recorded every second. The difference between the minimum and maximum temperature, ΔT, for the 10 highest and lowest values was averaged, and are listed in Table 2. The standard deviation of these values was less than 1% in all cases. The larger COV for the carbon steel is likely to derive from inhomogeneities, such as cementite (Fe_3C) present in the alloy, which ranges in size about to 25 μm. The 304L stainless steel is spatially homogeneous; cementite inclusions are of the order of 1 μm[8].

The differences in surface temperature could be reproduced through finite element modeling. Steady-state heat transfer to a medium is given by Fourier's law in two-dimensions as shown in Eq. 1

$$\frac{\partial^2 T}{\partial x^2} + \frac{\partial^2 T}{\partial y^2} = -\frac{q'''}{k} \tag{1}$$

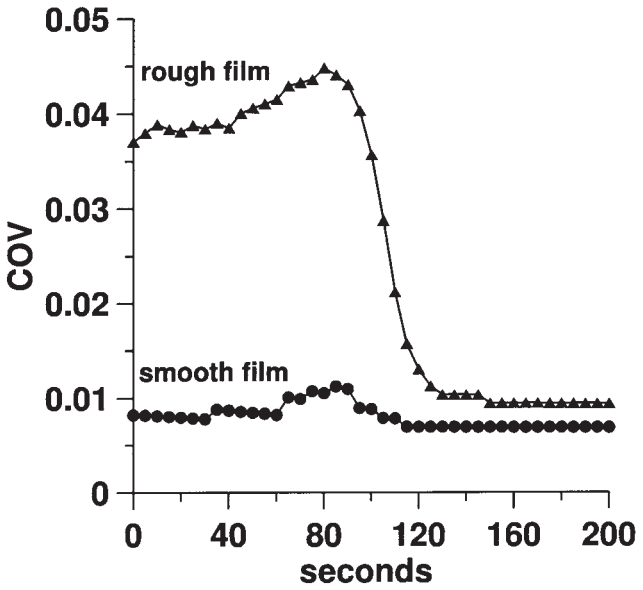

Figure 6. COV of the surface temperature during drying of a polyacrylate polymer film at 117 °C.

The smooth film is on stainless steel and the rough film is on carbon steel.

where T is temperature, x and y are dimensions in the plane of the coupon, q''' is the volumetric heat source, and k is the thermal conductivity. The surface of the metal was divided into 97×99 uniform volume elements in the x-y plane, which was close to the maximum grid size allowed by the computer program used[9]. Each element could be assigned a different thermal conductivity, which allowed the spatial variations in heat transfer of a composite material such as carbon steel to be modeled.

The x-y plane was modeled as a 2×2 cm area, so that the length of a low conductivity region was approximately 200 μm. Boundary conditions were set at the four edges of the grid and the relative thermal conductivity, λ_{rc}, ranging from zero to one was calculated with Eq. 2. Here, k_i is the thermal conductivity of material i, and k_{Fe} is the thermal conductivity of iron. The initial temperature was entered for each element. Equation 1 was solved for each element in the calculation grid using the modified strongly implicit iterative method described by Ribando[9]

$$\lambda_{rc} = \frac{k_i}{k_{Fe}} \tag{2}$$

Our first goal was to determine the temperature difference resulting from inclusion of a low conducting material, such as cementite or an iron oxide into a composite comprised primarily of iron. This simulation models a situation where a room temperature coupon is placed into a warm oven. The temperatures at the edges of the coupon were set at 80°C. Heating was assumed to occur from the edges of the coupon, which leads to the boundary condition: $T(x = 0, L; y = 0, W; t) = 80$°C. Both L and W were set at 2 cm as indicated earlier. The volumetric heat source term was iteratively changed with respect to the relative thermal conductivity until the change in temperature was less than 0.001% between iterations.

Lower-conducting inclusions were simulated by adding cells with lower conductivity values to the grid.[10] The external temperature was set at 105°C. Heating was simulated by adjusting the volumetric heat generation terms at the edge of the coupon until the average interior temperature equaled the oven temperature. Cells corresponding to λ_{rc} values of 0.1 and 0.3 regions were distributed equally and randomly across the surface so as to occupy 0.8% of the surface area. The ΔT (max temperature minus minimum temperature) value was 7.3°C in the $\lambda_{rc} = 0.1$ regions, and the $\lambda_{rc} = 0.3$ regions returned a ΔT value of 3.4°C. The average temperature is 79°C. The simulated ΔT values compare well with the experimental value of 5.3°C at 75°C. The calculated temperature distribution gave a COV value of 0.11. ΔT is also dependent on the size of the lower-conducting features in the metal surface. For example, increasing the doped area from 10 to 40 μm^2 doubles ΔT.

Surface driven flow

The differences in drying behavior between the films are proposed to be caused by variations in surface driven flow. Marangoni convection can result from surface tension gradients due to heterogeneous temperature distributions at the surface.[11] The surface of the film deposited on carbon steel becomes rough because of higher surface driven flow due to uneven heat transfer at the liquid/metal interface caused by the nonuniformity of the metal. This was quickly tested by marking the stainless steel surface with an ink marker (prior to applying the adhesive formulation) in order to disrupt the uniformity of heat transfer at the metal surface. The inhomogeneity introduced made the behavior of stainless steel approach that of carbon steel as shown in Figure 3. The temperature gradients appear to create surface tension gradients and induce thermal Marangoni flow.[12]

The Marangoni number (Ma) is defined in Eq. 3

$$Ma = \frac{\tau \Delta T D}{\mu \kappa} \tag{3}$$

where τ is the negative surface tension gradient with respect to temperature ($\tau = -\delta\sigma/\delta T$), ΔT is the difference in local temperature, D represents the thickness of fluid film, μ stands for the viscosity of the fluid, and κ is the thermal diffusivity.[13,14] The ΔT used to calculate the Ma number is the difference between the maximum and minimum temperature measured by IR thermography on the surface of the film during the initial stages of drying, which was taken as the first 10 s. Similar results were obtained when data from the first five or 20 s were used, except that the deviation in the data at 5 s (2.8%) was slightly greater than that (1.1%) measured at 10 or

Table 2. Temperature Differences (ΔT, °C) Measured during the Heating of Coupons

Drying Temperature (°C)	Carbon steel	Stainless steel	Silicon
75	5.3	4.9	3.1
90	5.7	4.0	3.4
105	7.3	4.9	3.9

20 s. The film thickness was assumed to be 40 μm, which is twice the measured value of the dry film. The viscosity of the adhesive formulation was 1.3×10^{-1} N-s/m^3 as provided by the manufacturer. The surface tension gradient of 1.7×10^{-2} N/m-°C[15], and the thermal diffusivity of 1.5×10^{-7} m^2/s[16] are those of water, but similar have been reported for aqueous polymer systems.[17-19] No temperature dependence is assumed in these values because the overall thermal response of the films does not change with the substrate on which they are deposited. The differences are on a length scale associated with the size of the impurities that lead to nonuniform heat transfer.

Marangoni numbers calculated at various temperatures show a general increase with drying temperature, which is consistent with the literature.[20,21] They are consistently higher for the films on carbon steel, which is expected because of nonuniform heat transfer. The marked stainless steel coupons lead to slightly higher Ma numbers for the two lower temperatures, compared to the stainless steel coupons. This is consistent with the temperature behavior observed with the marked coupons and derives from the interruption of heat transfer to the metal coupon by the ink. The separation of tacky material from the bulk formulation contributes to the difference in tack between the carbon steel and stainless steel-based films. The thermal gradients responsible for Marangoni flow would make the smaller constituents diffuse faster, which could lead to chemical separation.

In conclusion, order-of-magnitude differences in the tackiness of adhesive films can be developed by drying them on different metal supports. The magnitude of the difference rivals that of transitioning between ordered and isotropic polymer phases.[22] Contact angle measurements demonstrate that the polar component of the surface energy is associated with the difference in tack. Infrared thermography supported by finite element calculations show that the film deposited on carbon steel gives rise to a rougher surface as compared to an analogous film on stainless steel. AFM work confirms that the carbon steel-based film is rougher at the microscale and shows that the tacky component in the formulation separates into microscale valleys at the surface, where it is protected from surface-to-surface contact. The higher surface roughness for the carbon steel-based film arises from uneven heat transfer from the coupon to the adjoining liquid film because of components of low thermal conductivity present in carbon steel. The resulting difference in surface tension induces Marangoni flow, which is believed to be responsible for the surface roughness.

Acknowledgments

This study was funded by the Member Companies of the Institute of Paper Science and Technology.

Literature Cited

1. Russell T, Kim H. Tack-a sticky subject. *Science*. 1999;285(8):1219-1220.
2. Chiche A, Pareige P, Creton C. Role of surface roughness in controlling the adhesion of a soft adhesive on a hard surface. *CR Acad Sci Paris*. 2000;IV(1)1197-1204.
3. Creton C, Leibler L. How does tack depend on time of contact and contact pressure? *J Poly Sci B*. 1996;34:545-554.
4. Severtson SJ, Wang XP, Kroll MS. Development of environmentally benign pressure sensitive adhesive systems via modification of substrate properties. *Ind Eng Chem Res*. 2002;41(23):5668-5675.
5. Zosel, A. The effect of fibrillation on the tack of pressure sensitive adhesives. *Int J of Adhesion and Adhesives*. 1998;18:265-271.
6. Fowkes FM. Attractive forces at interfaces. *Ind Eng Chem*. 1964**;**56: 40-52.
7. Fike G, Abedi J, Banerjee S. Imaging the drying of surfaces by infrared thermography. *Ind Eng Chem Res*. 2004;43:4178-4181.
8. Mapelli C, Nolli P. Formation mechanism of non-metallic inclusions in different stainless steel grades. ISIJ International. 2003;43(8):1191-1199.
9. Ribando R. *Heat Transfer Tools*. Boston: McGraw Hill; 2002.
10. Fike GM. *Determination of polymer film development through surface characterization studies*. Georgia Institute of Technology; 2005: PhD Diss.
11. Pearson J. On convection cells induced by surface tension. *J Fluid Mech.* 1958;4:489-500.
12. Gugliotti M. Tears of Wine. *J Chem Ed*. 2004;81(1):67-68.
13. Ismagilov R, Rosmarin D, Gracias D, Stroock A. Competition of intrinsic and topographically imposed patters in Benard-Marangoni convection. *Appl Phys Letts*. 2001;79(3):439-441.
14. Char M-L, Chiang K.-T. Stability analysis of Benard-Marangoni convection in fluids with internal heat generation. *J of Phys D: Appl Phys*. 1994;27:748-755.
15. Perry R, Green D, Maloney J. eds. *Perry's Chemical Engineers' Handbook*. 6th ed. New York: McGraw-Hill; 1984.
16. Lide, D (Ed). CRC Handbook of Chemistry and Physics. 81st ed. Boca Raton: CRC Press; 2001.
17. Hansen C. New simple method to measure polymer surface tension. *Pigment & Resin Technol*. 1998;27(6):374-378.
18. Azab M, Bader S, Shaaban A. Nonionic surfactants based on copolymers of dioctyl itaconate with dioxypropylated itaconic acid. *Pigment & Resin Technol*. 2001;30(6):388-394.
19. Abramson E, Brown J, Slutsky L. The thermal diffusivity of water at high pressures and temperatures. *J Chem Phys*. 2001;115(22):10461-10463.
20. Birnie D. Combined flow and evaporation during spin coating of complex solutions. *J of Non-Crystalline Solids*. 1997;218:174-178.
21. Saylor J, Smith G, Flack K. An experimental investigation of the surface temperature field during evaporative convection. *Phys of Fluids*. 2001;13(2):428-439.
22. Pelacho M, Garcimartin A, Burguete J. Local Marangoni number at the onset of hydrothermal waves. *Physical Review E*. 2000;62:477-484.

Manuscript received Oct. 25, 2005, and revision received Feb. 4, 2006.